

**Theory of the isotropic-nematic transition in dispersions of compressible rods**

Kostya Shundyak

*Instituut-Lorentz for Theoretical Physics, Leiden University, Niels Bohrweg 2, 2333 CA Leiden, The Netherlands*

René van Roij

*Institute for Theoretical Physics, Utrecht University, Leuvenlaan 4, 3584 CE Utrecht, The Netherlands*

Paul van der Schoot

*Eindhoven Polymer Laboratories, Technische Universiteit Eindhoven, P.O. Box 513, 5600 MB Eindhoven, The Netherlands*

(Received 2 February 2006; published 24 August 2006)

We theoretically study the nematic ordering transition of rods that are able to elastically adjust their mutually excluded volumes. The model rods, which consist of a hard core surrounded by a deformable shell, mimic the structure of polymer-coated, rodlike fd virus particles that have recently been the object of experimental study [K. Purdy *et al.*, *Phys. Rev. Lett.* **94**, 057801 (2005)]. We find that fluids of such soft rods exhibit an isotropic-nematic phase transition at a density higher than that of the corresponding hard-rod system of identical diameter, and that at coexistence the order parameter of the nematic phase depends nonmonotonically on the elastic properties of the polymer coating. For binary mixtures of hard and soft rods, the topology of the phase diagram turns out to depend sensitively on the elasticity of a shell. The lower nematic-nematic critical point, discovered in mixtures of bare and polymer-coated fd virus particles, is not reproduced by the theory.

DOI: [10.1103/PhysRevE.74.021710](https://doi.org/10.1103/PhysRevE.74.021710)

PACS number(s): 61.30.Cz, 61.30.Vx, 64.70.Md, 61.25.Hq

**I. INTRODUCTION**

Recently developed methods to control the contour length and the effective diameter of elongated virus particles [1,2] have opened up the way to systematically study the bulk phase behavior of mono- and bidisperse rods over a relatively wide range of lengths and widths. This is important, because it allows for the experimental verification of a vast amount of theoretical work that has been done on the isotropic-to-nematic (*IN*) phase transition in dispersions of mutually repelling rods, and in particular that on bidisperse mixtures [3–8]. The agreement of theoretical predictions for binary dispersions with experimental data [9–14] has so far not been as impressive as that for monodisperse ones [15,16], where the impact of, e.g., the size [17], shape [18], molecular flexibility [19–21], and Coulomb interactions [22–24] appears to be well understood [7,25].

One of the reasons for this state of affairs is probably that in binary mixtures there is a coupling between ordering, fractionation, and demixing, leading to a much more complex phase behavior [7,8,26–28]. Indeed, in bidisperse systems more length scales compete with each other, presumably making them more sensitive to the effects of flexibility, residual van der Waals attractions, nonadditivity, or charges [5,29–32]. Binary mixtures are therefore a much more critical gauge of the accuracy of theories than monodisperse systems are. In some cases, the disagreement between theory and experiment is not just quantitative [16] but even qualitative. For example, in experiments on aqueous mixtures of bare fd virus particles and fd virus particles onto which polymeric chains are grafted, Purdy *et al.* [2] discovered a nematic-nematic coexistence region that exhibits a lower critical point. Extensions of Onsager's classical second-virial theory for infinitely rigid rods incorporating a diameter bidispersity do not predict such a lower critical point

[4,27,28,33], not even if one allows for nonadditivity of the interactions between the species [32]. However, these theories do predict a nematic-nematic demixing either with an upper critical point or no critical end point at all [8,28,34,35].

Theoretically, nematic-nematic demixing transitions of bidisperse rods with a lower critical end point have been predicted, but only for rods with a sufficiently large bending flexibility [37], or for sufficiently short rods for which higher-order virials become important [31,38–42]. It appears, however, that some of the predictions are quite sensitive to the invoked approximations, and in our view the issue remains contentious. For instance, depending on how precisely higher-order virials are approximately accounted for, the lower critical point appears and disappears in the phase diagram [43]. This is reminiscent of the qualitative difference in the predicted phase behavior of hard-rod mixtures, depending on whether the exact orientational distribution is used or a Gaussian approximation to that [8,28,34,35,44]. So, given the apparently inherent sensitivity to the details of the theories, it remains important to explore alternative explanations of the observed phase behavior, and in particular that of the lower critical end point.

A factor that has not been considered, and that could significantly influence the phase behavior in systems such as those studied by Purdy and co-workers, is the finite compressibility of the polymer coating of the rods. The effective diameter of these polymer-coated rods is not necessarily fixed but could well be a function of the thermodynamic state of the dispersion. So far, the dimensions of rodlike colloids have been treated as quenched variables, i.e., as invariants of the thermodynamic state of the suspension. (An exception to this is micellar rods with annealed length distribution [45].) With the polymer-coated rods of Ref. [2] in mind, it seems opportune to consider explicitly the elastic

response of this coating to the osmotic pressure of the dispersion. Contrary to, for instance, theoretical work on the crystallization of dendrimers, where entropic interactions of a similar nature are modeled by a soft potential [46], we model the effects of compression not at the interaction potential level but at the level of the volume exclusion. In effect, our theory is that of particles with an annealed diameter, and hence an annealed excluded volume.

Our calculations show that monodisperse fluids of elastically compressible rods exhibit an isotropic-nematic phase transition at a density higher than that of the corresponding incompressible-rod system of equal diameter, as expected. How much higher depends on the stiffness of the shell. Weakly impacted upon by the shell stiffness is the relative density gap in the coexisting phases. For binary mixtures of incompressible and compressible rods, the structure of the phase diagram changes dramatically with varying elasticity of the coating, showing once more the sensitivity of these kinds of mixtures to the details of the interactions [32]. Still, the topology of the phase diagrams that we calculate does bear some resemblance to that of incompressible hard-rod mixtures of unequal diameter: an upper but no lower nematic-nematic critical point is produced by the theory.

The remainder of this paper is organized as follows. In Sec. II, we first introduce the Onsager-type free-energy functional, and derive from that the basic Euler-Lagrange equations describing the orientational and density distribution of the elastically compressible rods under conditions of thermodynamic equilibrium. In Sec. III, we study the behavior of a monodisperse fluid of such compressible rods. In order to obtain an analytical solution to the model, we invoke a Gaussian approximation to the orientational distribution function. We compare this analytical theory with an exact, numerical evaluation and find fair agreement. In Sec. IV we analyze the bulk phase diagrams of binary mixtures of hard rods and elastically compressible ones, but now only numerically keeping in mind the sensitivity of the binary phase diagram to approximations invoked. A summary and discussion of the results are presented in Sec. V.

## II. DENSITY FUNCTIONAL AND METHOD

We are concerned with the bulk properties of a fluid of cylinders of two different species  $\sigma=1, 2$  of diameter  $D_\sigma$  and equal length  $L$  in a macroscopic volume  $V$  at temperature  $T$  and chemical potentials  $\mu_\sigma$ . We presume the limit  $D_\sigma/L \rightarrow 0$  to hold, in which case a second virial theory is believed to be exact [47]. The “effective” diameter  $D_1$  of the thin rod is determined by the bare hard core of the particle  $D_1 = \Delta^{\text{core}}$ , whereas the diameter of the thick (coated) rods is written as  $D_2(\gamma) = \Delta^{\text{core}} + \gamma \Delta^{\text{pol}}$ , with  $\Delta^{\text{pol}}$  twice the thickness of the soft polymeric shell. The compression factor  $\gamma \in [0, 1]$  parametrizes the deformation of this soft shell due to interactions with other rods in the system. At infinite dilution, we expect zero deformation of the thick rigid rod, i.e.,  $\gamma=1$ , and it is convenient to define the limiting diameter ratio  $d = D_2(\gamma=1)/D_1 = 1 + \Delta^{\text{pol}}/\Delta^{\text{core}}$ .

The compression of the grafted polymer layer reduces the excluded volume, as we will see explicitly below, at the ex-

pense of an elastic energy. Introducing the rigidity  $k$  of the polymeric shell, we write the elastic energy of a single rod at a compression equal to  $\gamma$  as  $k(\gamma^2 + \gamma^{-2} - 2)/2$  in units of thermal energy  $k_B T$ . It is inspired by the theory of ideal (Gaussian) polymers [36], where we presume that the grafted polymers are not strongly stretched [2]. Hence, we expect the numerical value of the rigidity  $k$  to be of order of the number of chains grafted onto each rod. However, for simplicity we presume it to be a free parameter. Note that for  $\gamma=1$ , the elastic contribution to the free energy is zero, as it should be.

The total grand potential  $\Omega[\rho_1, \rho_2]$  of the spatially homogeneous suspension is now written as a functional of the distribution functions  $\rho_\sigma(\mathbf{u})$ , where  $\mathbf{u}$  denotes the unit vector along the axis of a rod. The distributions are normalized such that  $\int d\mathbf{u} \rho_\sigma(\mathbf{u}) = n_\sigma$ , the number density of species  $\sigma$  at the imposed chemical potential. Within the second virial approximation, we write the functional as [7,15]

$$\begin{aligned} \frac{\beta\Omega[\{\rho_\sigma\}]}{V} = & \sum_\sigma \int d\mathbf{u} \rho_\sigma(\mathbf{u}) \{ \ln[\rho_\sigma(\mathbf{u}) \nu_\sigma] - 1 - \beta\mu_\sigma \} \\ & + \frac{1}{2} \sum_{\sigma\sigma'} \int d\mathbf{u} d\mathbf{u}' E_{\sigma\sigma'}(\mathbf{u}; \mathbf{u}') \rho_\sigma(\mathbf{u}) \rho_{\sigma'}(\mathbf{u}') \\ & + \frac{1}{2} k(\gamma^2 + \gamma^{-2} - 2) \int d\mathbf{u} \rho_2(\mathbf{u}), \end{aligned} \quad (1)$$

with  $\beta = (k_B T)^{-1}$  the inverse temperature,  $\nu_\sigma$  the thermal volume of the species  $\sigma$ , and the excluded volume due to hard-core interactions

$$E_{\sigma\sigma'}(\mathbf{u}, \mathbf{u}') = L^2 (D_\sigma + D_{\sigma'}) |\sin[\arccos(\mathbf{u} \cdot \mathbf{u}')]|, \quad (2)$$

where additional  $O(LD^2)$  terms are being ignored, in line with the needle limit ( $D_\sigma/L \rightarrow 0$ ) of interest here.

The equilibrium conditions on the functional,  $\delta\Omega[\{\rho_\sigma\}]/\delta\rho_\sigma(\mathbf{u})=0$  and  $\partial\Omega[\{\rho_\sigma\}]/\partial\gamma=0$ , lead to the set of nonlinear integral equations,

$$\begin{aligned} \beta\mu_\sigma = & \ln[\rho_\sigma(\mathbf{u}) \nu_\sigma] + \sum_{\sigma'} \int d\mathbf{u}' E_{\sigma\sigma'}(\mathbf{u}, \mathbf{u}') \rho_{\sigma'}(\mathbf{u}') \\ & + \frac{1}{2} \delta_{\sigma,2} k(\gamma^2 + \gamma^{-2} - 2), \\ 0 = & k(\gamma - \gamma^{-3}) \int d\mathbf{u} \rho_2(\mathbf{u}) \\ & + \frac{1}{2} \sum_{\sigma\sigma'} \int d\mathbf{u} d\mathbf{u}' \frac{\partial E_{\sigma\sigma'}(\mathbf{u}, \mathbf{u}')}{\partial\gamma} \rho_\sigma(\mathbf{u}) \rho_{\sigma'}(\mathbf{u}'), \end{aligned} \quad (3)$$

to be satisfied by the equilibrium distributions. The  $\gamma$  derivative in the last line involves the  $\gamma$  dependence of  $D_2$  through Eq. (2). These equations can be solved, either approximately within a Gaussian approximation or numerically on a grid of orientations. Details of the numerical schemes have been discussed elsewhere [28,33]. Here, in order to find the bulk uniaxially symmetric distributions  $\rho_\sigma(\theta_i)$ , with  $\theta = \arccos(\mathbf{u} \cdot \mathbf{n})$  the angle between the rod unit vector  $\mathbf{u}$  and the nematic director  $\mathbf{n}$ , we use a nonequidistant  $\theta$ -grid of

$N_\theta=30$  points  $\theta_i \in [0, \pi/2]$ ,  $1 \leq i \leq N_\theta$ , with 2/3 of them uniformly distributed in  $[0, \pi/4]$ . The resulting distributions can be inserted into the functional to obtain the grand potential  $-pV$ , with  $p$  the pressure. Then the complete thermodynamics can be inferred, as well as the phase diagram.

### III. MONODISPERSE SOFT RODS

As demonstrated in Refs. [7,15], the  $IN$  transition in suspensions of rigid rods is a result of a competition between the orientational entropy and the packing entropy (free volume). In order to estimate the impact of the elastic term of Eq. (1) on the  $IN$  transition, we first restrict our attention in this section to a purely monodisperse system of coated rods. Formally, this can be achieved by considering the limit  $\beta\mu_1 \rightarrow -\infty$  and  $\rho_1(\mathbf{u})L^2D_1 \rightarrow 0$  in the functional and its minimum conditions, and in this paragraph we drop the species index “2” for convenience.

First, instead of numerically solving for the minimum conditions, we adopt a Gaussian ansatz for the one-particle distribution function in the nematic phase, with  $\rho(\mathbf{u}) \propto \exp(-\alpha\theta^2/2)$  for  $\theta \leq \pi/2$  and  $\rho(\mathbf{u}) \propto \exp[-\alpha(\pi-\theta)^2/2]$  for  $\theta \geq \pi/2$ . Here,  $\alpha$  denotes a variational parameter that we fix by minimizing the free energy. From Eqs. (3) we obtain the following relations between the density and the compression in the isotropic phase  $I$ , where  $\alpha \equiv 0$ , and in the nematic phase  $N$ , where  $\alpha = 4c_N^2/\pi$  in terms of the dimensionless concentration  $c_N$  defined below,

$$\beta\mu_I = \ln c_I + 2c_I \frac{D(\gamma_I)}{D(1)} + \frac{1}{2}k(\gamma_I^{-2} + \gamma_I^2 - 2), \quad (4a)$$

$$c_I = \frac{kD(1)}{\Delta^{\text{pol}}}(\gamma_I^{-3} - \gamma_I), \quad (4b)$$

$$\beta\mu_N = 3 \ln c_N + 2 \ln \left( \frac{D(\gamma_N)}{D(1)} \right) + \frac{k}{2}(\gamma_N^{-2} + \gamma_N^2 - 2) + C, \quad (4c)$$

$$2 = \frac{kD(\gamma_N)}{\Delta^{\text{pol}}}(\gamma_N^{-3} - \gamma_N), \quad (4d)$$

with  $C = 2 \ln 2\pi^{-1/2} + 3$ ,  $c_{I(N)} = (\pi/4)n_{I(N)}L^2D(1)$  the dimensionless number density of the  $I(N)$  phase,  $D(\gamma) = \Delta^{\text{core}} + \gamma\Delta^{\text{pol}}$  the effective diameter of the coated rods, and  $D(1) = \Delta^{\text{core}} + \Delta^{\text{pol}}$ . In addition, the dimensionless pressures  $p^* = (\pi/4)\beta pL^2D(1)$  of the isotropic and nematic phases can be written as

$$p_I^* = c_I \left( 1 + c_I \frac{D(\gamma)}{D(1)} \right), \quad p_N^* = 3c_N. \quad (5)$$

Note that in the isotropic phase (i) the compression  $\gamma_I$  decreases monotonically with increasing  $c_I$  [see Eq. (4b)], and (ii) the elastic contribution to the free energy grows with increasing density, as one might in fact expect. More interestingly, in the nematic phase the rigidity and geometric parameters of the rods fully determine their compression [see

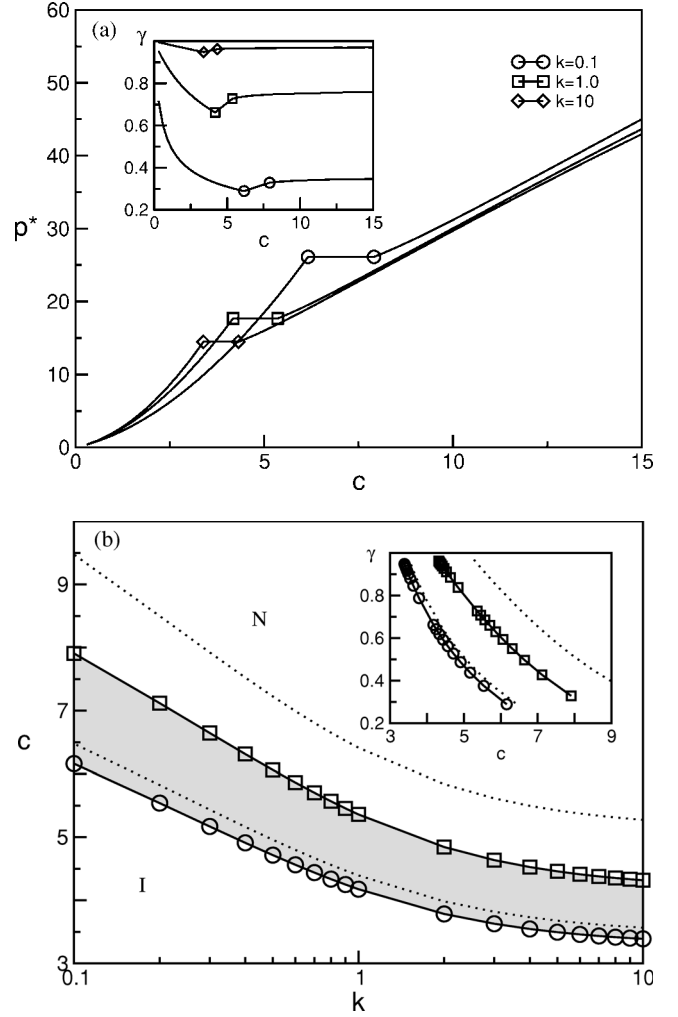


FIG. 1. (a) Equation of state for a fluid of monodisperse soft rods ( $d=1+\Delta^{\text{pol}}/\Delta^{\text{core}}=3$ ) in terms of the dimensionless bulk pressure  $p^*=(\pi/4)\beta pL^2D(1)$  and the dimensionless density  $c=(\pi/4)nL^2D(1)$  for several values of shell rigidities  $k=0.1, 1.0, 10$ . The inset shows the dependence of the compression factor  $\gamma$  on density  $c$  for the same values of  $k$  as in the main plot. (b) Bulk phase diagram for the same system in  $c$ - $k$  coordinates. The coexistence region (gray area) separates regions of the isotropic ( $I$ ) and nematic ( $N$ ) phase, and the tie-lines connecting coexisting phases are vertical. The dotted lines indicate the corresponding coexistence  $IN$  curve, calculated with the Gaussian trial function [Eqs. (4) and (5)]. The inset shows the dependence of the compression factors  $\gamma_{I,N}$  on density  $c$  at  $IN$  coexistence for the same range of  $k$  as in the main plot.

Eq. (4d)], which is independent of concentration (at the level of the Gaussian approximation). Hence, in the nematic phase the contribution of the elastic compression can be considered as an effect of a uniform bulk field that renormalizes the value of the chemical potential. This is also consistent with the expression for the pressure of the nematic phase, which is only indirectly affected by the elasticity of the polymer coating of the rods. Overall, the elastic term shifts the  $IN$  transition to higher densities due to reduction of the effective diameter  $D(\gamma)$ . The results of our calculations are shown in Fig. 1 for the system with  $d=3$ , and other values of  $d$  lead to

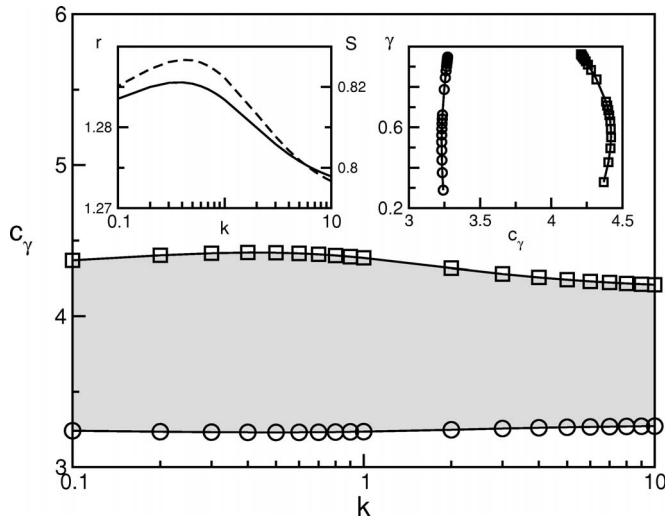


FIG. 2. The same bulk phase diagram as in Fig. 1(b) in terms of the scaled density  $c_\gamma = (\pi/4)nL^2D(\gamma)$  vs rigidity of the polymeric shell  $k$ . The right inset shows the dependence of the compression factor  $\gamma$  on the density  $c_\gamma$  for the same values of  $k$  as in the main plot. The left inset shows the ratio  $r = c_{\gamma,N}/c_{\gamma,I}$  of the densities of coexisting  $N$  and  $I$  phases (solid line) and the nematic order parameter  $S$  (dashed line) as a function of  $k$ . The right inset gives the compression  $\gamma$  of the rods in the coexisting phases, as a function of  $c_\gamma$ .

similar phase diagrams.

In Fig. 1(a), we show the dependence of the dimensionless bulk pressure  $p^*$  on the dimensionless number density  $c$  (i.e., the equation of state) for several values of rigidity  $k$  of the polymeric shell of the rod. The solid lines represent direct numerical solutions of Eqs. (3). The results of calculations within the Gaussian approximation are quite close to those from our numerical calculations, albeit that they overestimate the rod density in the coexisting isotropic and nematic phases by about 5% and 20%, respectively (not shown here for the sake of clarity) [7].

Imposing conditions of mechanical and chemical equilibrium between isotropic and nematic phase, we calculated the densities and the compression factors of the rods in the  $I$  and  $N$  phases at coexistence, and present these in Fig. 1(b) for the realistic range of rigidities of  $k \in [0.1, 10]$ . The dotted lines give the results of the calculations within the Gaussian approximation, whereas the numerical solutions to Eqs. (3) are represented by the symbols, with the solid lines serving as a guide to the eye. While the predictions for the concentration of rods in the isotropic phase at coexistence are in almost quantitative agreement, those for the phase gap are not: the Gaussian approximation overestimates the phase gap by a factor of about 2. For rigidities of order  $k \approx 10$ , the limiting densities  $c_{IN}$  of the coexisting phases approach the values of the corresponding hard rod system. The polymeric shells of the rods are then only slightly deformed ( $\gamma \approx 1$ ). On the other hand, in the limit of small  $k$ , the densities at coexistence approach those of hard rods with the smaller hard-core diameter  $\Delta^{\text{core}}$ , because in that case  $\gamma \rightarrow 0$ . The leveling off occurs only for very small values of  $k$ , and is not shown in Fig. 1(b). The compression factors  $\gamma_{I,N}$  of the rods in the

coexisting phases are shown in the inset. The values calculated within the Gaussian approximation are similar to those obtained from our numerical analysis. Again, in the isotropic phase the agreement is almost quantitative.

It is clear from Fig. 1 that the dimensionless density  $c$  at the  $IN$  transition increases with a softening of the polymer layer, which of course is not all that surprising. From a theoretician's point of view,  $c = (\pi/4)nL^2D(1)$  is indeed the preferable concentration scale, because it does not depend explicitly on  $\gamma$ . The question now arises whether experimentally the bare diameter  $D(1)$  of the rods might be determined from the actual concentration of particles at which the nematic phase appears [7,25]. The answer appears to be negative, because the actual diameter will not have this value at the point where the nematic phase becomes stable. If  $D(1)$  were determined independently, e.g., from the compressibility at low concentrations, then this would allow one to obtain a value for  $k$ .

Theoretically, the structure of Eqs. (4) and (5), hints at the usefulness of the scaled densities  $c_\gamma = (\pi/4)nL^2D(\gamma)$ , and it is instructive to compare both density representations because it helps to explain the underlying physics. The phase diagram of Fig. 1 redrawn in terms of  $\{c_\gamma, k\}$  is shown in Fig. 2. It suggests that the density variation with  $k$  at the  $IN$  transition mainly comes from the reduction of the effective diameter  $D(\gamma)$  the rods. This conclusion is supported by the similarity of the values of the compression  $\gamma_{I,N}$  of the polymer shells of the rods in the coexisting phases, the dependencies of which on the density  $c_\gamma$  are presented in the right inset in Fig. 2.

Finally, several other quantities can be useful for qualitative comparisons with experiments. In the left inset in Fig. 2 we present the density ratio  $r = c_{\gamma,N}/c_{\gamma,I}$  of the  $I$  and  $N$  phases

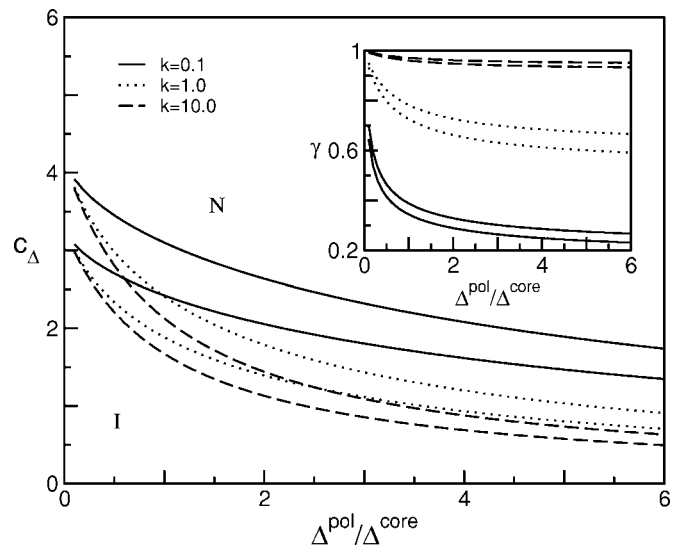


FIG. 3. Bulk phase diagrams in terms of the dimensionless density  $c_\Delta = (\pi/4)nL^2\Delta^{\text{pol}}$  vs relative thickness of the polymeric shell  $\Delta^{\text{pol}}/\Delta^{\text{core}}$  for rods with several rigidities  $k=0.1, 1.0$ , and  $10$ . The inset shows the dependence of the compression factors  $\gamma$  in coexisting phases on  $\Delta^{\text{pol}}/\Delta^{\text{core}}$  for the same values of  $k$  as in the main plot.

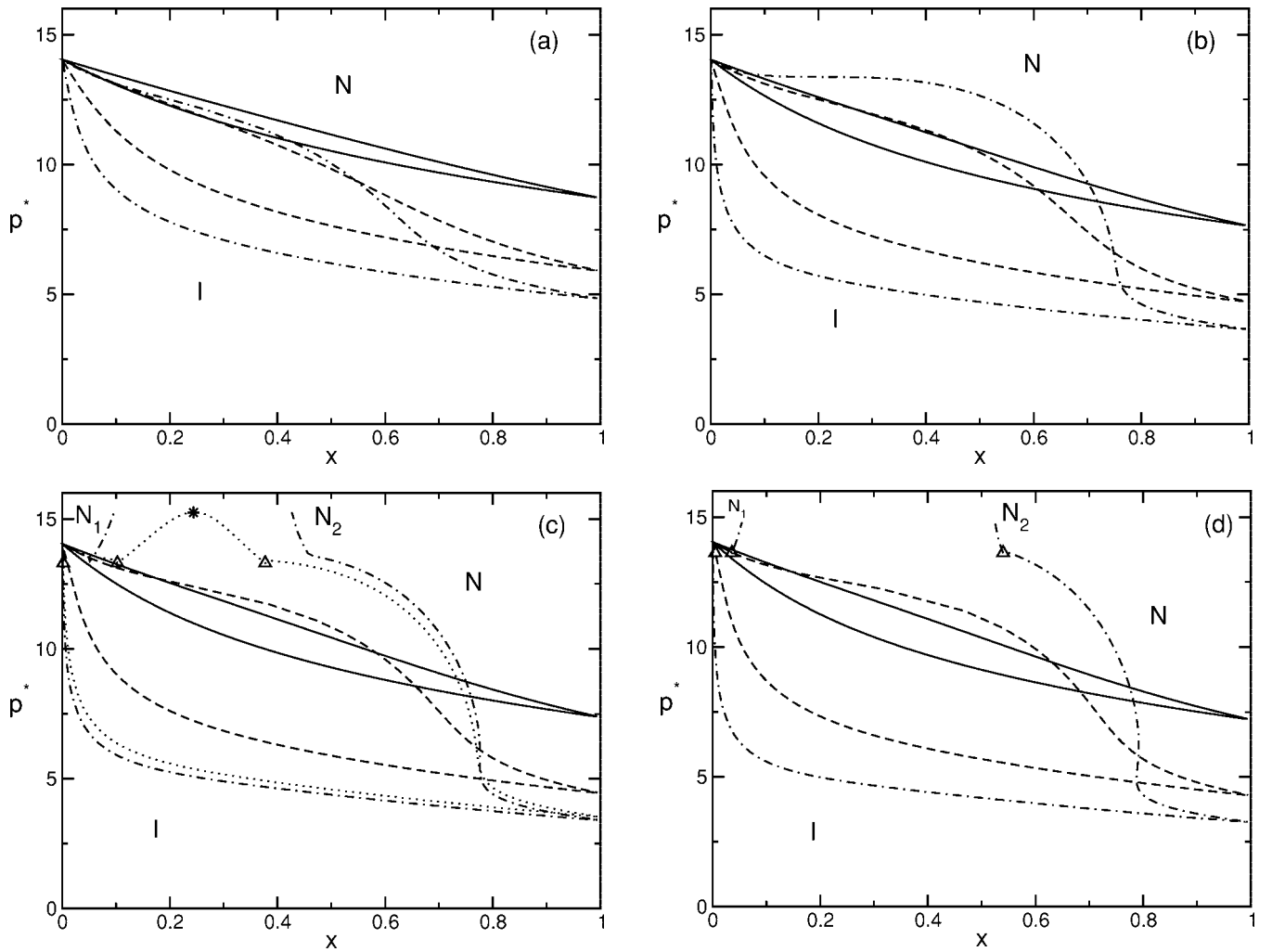


FIG. 4. Bulk phase diagrams of binary mixtures of hard ( $\Delta_1^{\text{pol}}=0$ ) and soft rods  $d=3.0$  (a),  $4.0$  (b),  $4.3$  (c), and  $4.5$  (d) in terms of the dimensionless pressure  $p^*=(\pi/4)\beta p L^2 \Delta^{\text{core}}$  and the composition  $x=n_2/(n_1+n_2)$  for different rigidities:  $k=0.1$  (solid),  $k=1.0$  (dashed),  $k=5.0$  [dotted, only in (c)], and  $k=10$  (dot-dashed). In (c, d),  $\Delta$  indicate the isotropic  $I$  and nematic  $N_1, N_2$  phases of different composition at coexistence, and the  $NN$  remixing point in (c) is marked with  $*$ .

at coexistence, as well as the nematic order parameter  $S$  as a function of the rigidity  $k$ . The dependence of  $c_N/c_I$  of the unscaled densities on  $k$  is similar to that of  $c_{\gamma,N}/c_{\gamma,I}$ , and is not shown here. The small variations of  $c_{\gamma,N}/c_{\gamma,I}$  and  $S$  with  $k$  indicate that in experiments it would be quite hard to use these two quantities to determine the shell rigidity  $k$ .

Variation of the molecular weight of polymer that forms the shells of the rods allows for a modification of its thickness  $\Delta^{\text{pol}}$ . In Fig. 3, we show several bulk phase diagrams in terms of the dimensionless densities  $c_\Delta=(\pi/4)nL^2\Delta^{\text{core}}$  and the ratio  $\Delta^{\text{pol}}/\Delta^{\text{core}}$  for systems with rigidities  $k=0.1, 1,$  and  $10$ . Note that our previous definition of the scaled density  $c=(\pi/4)nL^2D(1)$  [as in Eqs. (4) and (5), and Fig. 1] would be inconvenient here, as it contains explicit dependence on  $\Delta^{\text{pol}}$ . At the smallest studied thickness of the polymeric shell,  $\Delta^{\text{pol}}/\Delta^{\text{core}}=0.1$  densities  $c_{\Delta,IN}$  closely approach correspondent values for monodisperse hard rods. As the thickness of the shell increases, the transition densities  $c_{\Delta,IN}$  decrease as one would in fact expect. The inset in Fig. 3 shows the variation with the shell thickness of the compression factors  $\gamma_{I,N}$

for the same  $k$ 's as in the main plot. It appears that the compression of the shells increases for larger values of  $\Delta^{\text{pol}}$ .

#### IV. BINARY MIXTURES

For binary mixtures of soft rods, the effective diameters  $D_\sigma(\gamma)$  are different, and one can expect significant modifications of the phase behavior in comparison with the hard-rod binary fluids. We study the bulk properties of mixtures of bare hard and coated soft rods with  $d=3.0, 4.0, 4.3,$  and  $4.5$  for various values of  $k$ , chosen to mimic the experiments of Ref. [2]. Before presenting results of our calculations, it is useful to recall the structures of the bulk phase diagrams of hard-rod mixtures, i.e., of mixtures of incompressible rods with different diameters. For all values of the parameter  $d$ , they exhibit a low-density  $I$  phase, which at some intermediate values of densities separates into coexisting  $I$  and  $N$  phases with different composition. In mixtures with  $d<4.0$ , the high-density region has a single  $N$  phase, whereas for the systems with  $d\geq 4.0$  this  $N$  phase can demix into two differ-

ent nematics  $N_1, N_2$  (depending on the composition). The diameter ratio  $d$  of the species also determines whether this  $NV$  phase separation persists to (arbitrary) high densities ( $d > 4.2$ ), or whether these  $N_1, N_2$  phases remix back [7,34,35].

The phase diagrams of the “soft-hard” mixtures were determined by solving Eqs. (3) under conditions of mechanical and chemical equilibrium. We have verified that an artifact resulting from the discretization of the angular degrees of freedom of the rods, and that produces a nematic phase of perfect orientational order, does not interfere with our calculations [48].

The results of the calculations are shown in Fig. 4, where we give the bulk phase diagrams of the mixtures in terms of the dimensionless pressure  $p^* = (\pi/4)\beta p L^2 \Delta^{\text{core}}$  and composition  $x = n_2/(n_1 + n_2)$  for different rigidities  $k$ . In this representation, the tie lines connecting coexisting state points are horizontal because they correspond to the equal pressure condition. There are several features of the bulk phase diagrams that we would like to point out.

(i) For all diameter ratios  $d$  of mixtures of hard and very soft rods ( $k \sim 0.1$ ), the pressure  $p^*$  at coexistence varies almost linearly with composition  $x_N$  of the nematic phase. Detailed numerical evaluations show that  $p^*$  depends approximately linearly on the total density of the mixture  $n = n_1 + n_2$ , which is reminiscent of the behavior of a monodisperse system. This is to be expected, because there is only a weak coupling then to the elastic response of the soft component. In our calculations, both hard and soft rods have a hard core of equal diameter.

(ii) For a given value of  $d$ , the phase gap at  $IN$  coexistence is significantly smaller for systems with smaller values of  $k$  than that for large  $k$ . A large phase gap is usually seen as indicative of polydispersity effects. Interestingly, a narrow  $IN$  phase gap was observed in the experiments with PEG-coated fd-viruses [2], much narrower than to be expected if both components were indeed incompressible.

(iii) Although a rigidity of  $k=10$  seems high and should render the mixture close to that of hard rods of unequal diameter, as can be inferred from our results on monodisperse rods in Sec. III, an  $N_1 N_2$  phase separation is not observed for  $d=4.0$ . We recall that it does manifest itself in rigid hard-rod mixtures of this diameter ratio [28,33]. Such a strong sensitivity of the stability of the nematic phase on the elasticity of the shell is also seen in Fig. 4(c), where an increase of the rigidity from  $k=5$  to 10 hardly affects the  $IN$  transition curves, whereas it does prevent the  $N_1 N_2$  remixing at high pressures in the  $k=10$  case.

Finally, in Fig. 5 we show the compression factor  $\gamma_{I,N}(x)$  of the polymeric shells of the rods in the coexisting  $I$  and  $N$  phases for  $k=0.1, 1, 5$ , and 10 for  $d=4.3$ , as a function of the mole fraction  $x$ . Mixtures with other values of  $d$  and  $k$  produce similar curves. Upon an increase of the relative concentration  $x$  of the soft rods, compression of the polymer shells increases monotonically, which reflects the proportionality of the elastic energy to  $x$ . Note that  $\gamma_I(x) < \gamma_N(x)$  for all the systems studied. Almost linear curves  $\gamma_{I,N}(x)$  for extremely soft rods ( $k=0.1$ ) again indicate effectively monodisperse behavior.

## V. SUMMARY AND DISCUSSION

In this paper, we have explored the bulk phase diagrams of monodisperse compressible rods and those of binary mixtures of incompressible and compressible rods. Our motivation for this is the experiments by Purdy and co-workers, in which polymer-coated fd virus particles were mixed with bare fd in aqueous suspension [2]. Not surprisingly, our study shows that a pure system of coated rods, modeled here by an elastically responding excluded-volume interaction, requires a higher number density to obtain a nematic phase than that of incompressible rods of equal diameter. Nevertheless, the density ratio of the rods in the coexisting phases remains very close to that of the pure hard-rod system, being 1.274. The same, in fact, is true for the nematic order parameter. This implies that these dimensionless quantities cannot be used to estimate the elastic modulus  $k$  of the polymer coating. For known values for the coat thickness,  $\Delta^{\text{pol}}$ , and the bare core diameter,  $\Delta^{\text{core}}$ , that of the modulus  $k$  might be calculated from the observed absolute density in either coexisting phase, using, e.g., Fig. 1 if  $\Delta^{\text{pol}}/\Delta^{\text{core}}=2$ .

The situation is very different when it comes to mixtures of compressible and incompressible rods, which we have investigated for relative coat thicknesses in the range of values equal to  $d=1 + \Delta^{\text{pol}}/\Delta^{\text{core}}=3.0, 4.0, 4.3$ , and 4.5. We find that the topology of the phase diagram in the pressure-composition representation changes quite dramatically in this small range of  $d$  values, with  $0.1 \leq k \leq 10$ . Upon an increase of the shell rigidity from the lowest to the highest value, we find (i) that the degree of fractionation at  $IN$  coexistence increases, and (ii) that the  $NV$  binodal, if present, changes from domelike to chimneylike, i.e., the upper critical point moves to infinite pressures at a critical value of  $k$  that depends on  $d$ . For conditions where there is an upper critical point in the phase diagram, we did not find a reentrant  $NN$

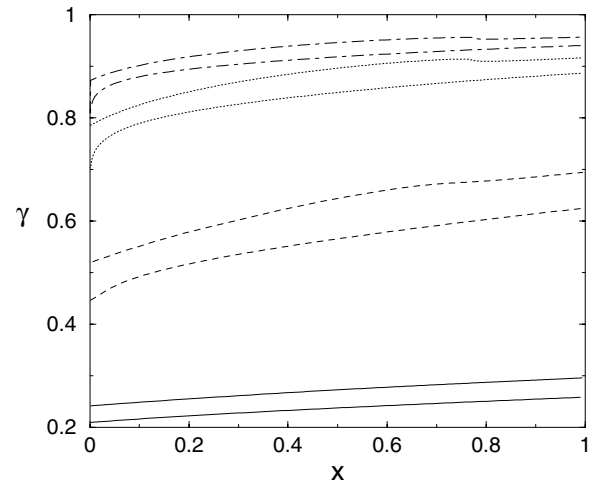


FIG. 5. Compression factors  $\gamma$  as a function of the mole fraction  $x$  in the coexisting isotropic (lower curve of each pair) and nematic (upper curve of each pair) phases in the binary mixture with  $d=4.3$ . Different pairs of curve correspond from bottom to top to increasing values of the rigidity  $k=0.1, 1.0, 5.0$  and 10. See also Fig. 4(c).

phase separation at higher pressures, i.e., no lower critical  $NV$  point was found. Therefore, the experimentally observed lower critical point cannot be explained by a compressible polymer coating, at least not within an Onsager type of approach.

As it is now clear that the phase behavior of the rods depends sensitively on the presence and properties of a polymeric coating, we suggest that a realistic model of any experimental system involving coated rodlike particles should not only correct for a finite bending rigidity and/or finite

length, but also for the elastic softness of that coating. We intend to pursue this in the near future.

#### ACKNOWLEDGMENTS

This work is part of the research program of the “Stichting voor Fundamenteel Onderzoek der Materie (FOM),” which is financially supported by the “Nederlandse organisatie voor Wetenschappelijk Onderzoek (NWO).”

- 
- [1] Z. Dogic and S. Fraden, *Philos. Trans. R. Soc. London, Ser. A* **359**, 997 (2001).
- [2] K. R. Purdy, S. Varga, A. Galindo, G. Jackson, and S. Fraden, *Phys. Rev. Lett.* **94**, 057801 (2005).
- [3] A. Abe and P. Flory, *Macromolecules* **11**, 1122 (1978).
- [4] H. N. W. Lekkerkerker, Ph. Coulon, R. Van Der Haegen, and R. Deblieck, *J. Chem. Phys.* **80**, 3427 (1984).
- [5] T. Odijk, *Macromolecules* **19**, 2313 (1986).
- [6] M. Birshtein, B. I. Kolegov, and V. A. Pryamitsin, *Vysokomol. Soedin., Ser. A* **30**, 348 (1988); *Polym. Sci. U.S.S.R.* **30**, 316 (1988).
- [7] G. J. Vroege and H. N. W. Lekkerkerker, *Rep. Prog. Phys.* **55**, 1241 (1992), and references therein.
- [8] A. Speranza and P. Sollich, *J. Chem. Phys.* **117**, 5421 (2002).
- [9] T. Itou and A. Teramoto, *Macromolecules* **17**, 1419 (1984).
- [10] T. Itou and A. Teramoto, *Polym. J. (Tokyo, Jpn.)* **16**, 779 (1984).
- [11] T. Sato, N. Ikeda, T. Itou, and A. Teramoto, *Polymer* **30**, 311 (1989).
- [12] T. Sato and A. Teramoto, *Acta Polym.* **45**, 399 (1994).
- [13] M. P. B van Bruggen, F. M. van der Kooij, and H. N. W. Lekkerkerker, *J. Phys.: Condens. Matter* **8**, 9451 (1996).
- [14] F. M. van der Kooij and H. N. W. Lekkerkerker, *Phys. Rev. Lett.* **84**, 781 (2000).
- [15] L. Onsager, *Ann N. Y. Acad., Ann. N.Y. Acad. Sci.* **51**, 627 (1949).
- [16] T. Sato and A. Teramoto, *Adv. Polym. Sci.* **126**, 85 (1996).
- [17] D. Frenkel, *J. Phys. Chem.* **91**, 4912 (1987); **92**, 5314 (1988).
- [18] P. Bolhuis and D. Frenkel, *J. Chem. Phys.* **106**, 666 (1997).
- [19] T. Itou and A. Teramoto, *Polym. J. (Tokyo, Jpn.)* **20**, 1049 (1988).
- [20] T. Itou and A. Teramoto, *Macromolecules* **21**, 2225 (1988).
- [21] D. DuPre and Shi-jun Yang, *J. Chem. Phys.* **94**, 7466 (1991).
- [22] T. Sato and A. Teramoto, *Physica A* **176**, 72 (1991).
- [23] I. I. Potemkin, R. E. Limberger, A. N. Kudlay, and A. R. Khokhlov, *Phys. Rev. E* **66**, 011802 (2002).
- [24] I. I. Potemkin, N. N. Oskolkov, A. R. Khokhlov, and P. Reineker, *Phys. Rev. E* **72**, 021804 (2005).
- [25] S. Fraden, in *Observation, Prediction and Simulation of Phase Transitions in Complex Fluids*, edited by M. Baus *et al.* (Kluwer, Dordrecht, 1995), p. 113.
- [26] R. Sear and G. Jackson, *J. Chem. Phys.* **103**, 8684 (1995).
- [27] R. van Roij and B. Mulder, *J. Chem. Phys.* **105**, 11237 (1996); **109**, 1584 (1998).
- [28] R. van Roij, B. Mulder, and M. Dijkstra, *Physica A* **261**, 374 (1998).
- [29] R. R. Matheson and P. J. Flory, *Macromolecules* **14**, 954 (1981).
- [30] R. Holyst and M. Schick, *J. Chem. Phys.* **96**, 721 (1992).
- [31] P. van der Schoot and T. Odijk, *J. Chem. Phys.* **97**, 515 (1992).
- [32] K. Shundyak, R. van Roij, and P. van der Schoot, *J. Chem. Phys.* **122**, 094912 (2005).
- [33] K. Shundyak and R. van Roij, *Phys. Rev. E* **68**, 061703 (2003).
- [34] G. J. Vroege and H. N. W. Lekkerkerker, *J. Phys. Chem.* **97**, 3601 (1993).
- [35] R. van Roij and B. Mulder, *Europhys. Lett.* **34**, 201 (1996).
- [36] A. Y. Grosberg and A. R. Khokhlov, *Statistical Physics of Macromolecules* (AIP Press, New York, 1994).
- [37] A. N. Semenov and A. V. Subbotin, *Vysokomol. Soedin., Ser. A* **31**, 2062 (1989); *Polym. Sci. U.S.S.R.* **31**, 2266 (1989).
- [38] J. P. Straley, *Mol. Cryst. Liq. Cryst.* **22**, 352 (1973).
- [39] H. H. Wensink, G. J. Vroege, and H. N. W. Lekkerkerker, *J. Phys. Chem. B* **105**, 10610 (2001).
- [40] S. Varga, A. Galindo, and G. Jackson, *Mol. Phys.* **101**, 817 (2003).
- [41] S. Varga, K. Purdy, A. Galindo, S. Fraden, and G. Jackson, *Phys. Rev. E* **72**, 051704 (2005).
- [42] R. van Roij (unpublished).
- [43] K. Shundyak and R. van Roij (unpublished).
- [44] P. C. Hemmer, *Mol. Phys.* **96**, 1153 (1999).
- [45] P. van der Schoot and M. E. Cates, *Langmuir* **10**, 670 (1994).
- [46] A. Jusufi, M. Watzlawek, and H. Löwen, *Macromolecules* **32**, 4470 (1999).
- [47] It was proven in [15] for the isotropic phase, and generally accepted for the nematic phase. See, e.g., [7].
- [48] K. Shundyak and R. van Roij, *Phys. Rev. E* **69**, 041703 (2004).